

Braking Performance Improvement for Hybrid Electric Vehicle Based on Electric Motor's Quick Torque Response

Takahiro Okano, Shin-ichiro Sakai, Toshiyuki Uchida, Yoichi Hori

Abstract

Electric motors have much better response characteristics than hydraulic actuators, and can generate rapid and continuous output torque. But conventional Hybrid Electric Vehicles do not make use of these excellent characteristics.

By utilizing electric motors, we can compensate for the error in hydraulic actuators, and realize the ideal Anti-lock Braking System. But the capacity of the electric motor in Hybrid Electric Vehicles is small, so the electric motor cannot produce sufficient braking torque. By designing cooperative braking control of the hydraulic actuator and electric motor, we can realize excellent ABS which we name Hybrid-ABS.

By combining these control methods, we propose a novel methods of motion control in Hybrid Electric Vehicle(HEV).

keywords: Hybrid Electric Vehicle, Control System, Anti-lock Braking System, Active Safety, Regenerative Braking, Smart Braking.

1 Introduction

Nowadays, we see a lot of Hybrid Electric Vehicles(HEV) like Prius[1] and Insight[2] on the road. The main aim of HEV has mainly been on fuel cost and environmental problem. From this point of view, HEV is superior to other next generation power-trains such as Pure Electric Vehicle(PEV) and Fuel Cell Electric Vehicle(FCEV)[3]. However we overlook other advantages of the electric motor in HEVs. These advantages can be summarized as follows,:

1. Electric motor can generate bi-directional torque (accelerating and decelerating) very quickly and accurately.
2. Motor torque can be measured easily.
3. More than one electric motor can be mounted on each EV.

In conclusion, these advantages of the electric motor give rise to the possibility of vehicle motion control in HEVs and EVs. Electrical engineering can contribute much to the theme. We have previously proposed motion control methods and road condition estimation methods[5]. In this paper, we propose an overall concept of motion control in HEV using the superior characteristics of electric motor.

2 Classification of vehicle stability control

Vehicle motion control can be classified into linear and non-linear region of tire characteristics which is described in Fig.1. To control the vehicle lateral motion, we must control each wheel independently. But present HEV has only one or two motors (in front and rear). So vehicle lateral motion control of HEV is difficult. But in vehicle longitudinal motion control, we can utilize the merits of electric motor, applications like "Super TCS"(function as both ABS and TCS) is possible. In this paper, we propose the integration vehicle motion control in longitudinal region of HEV.

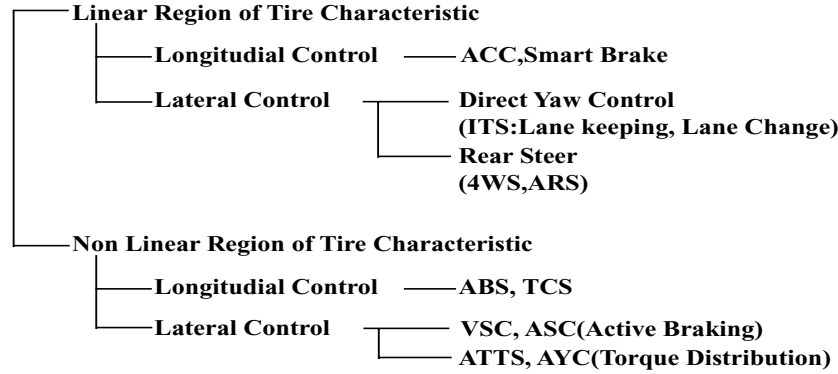


Fig. 1: Classification of vehicle stability control



Fig. 2: Our overall concept of motion control in Hybrid Electric Vehicle

Fig.2 shows the integrated braking control system for HEV with “electric motor’s fast feed back loop”. This system consists of three blocks. Each block has its own feedback loop. The most minor loop is the nominalization of hydraulic brake. The outer loops consist of Hybrid-ABS or vehicle velocity pattern shaping.

3 Nominalizaion of hydraulic brake by compensation of electric motor

The fatal weak point of the hydraulic brake is that we can not comprehend the braking/driving force between the tire and road’s surface. This point is not serious during normal driving by human, because human command will compensate for the error of the hydraulic brake. But in an emegency situation, hydraulic brake is controlled by the on-board computer. So error in hydraulic brake will be a fatal matter.

On the contrary, electric motor’s output torque can be measured easily. Using this point, we can construct a “braking/driving force observer” in EV. But HEV has both hydraulic brake and electric motor. In this mixed system, we can not construct “braking/driving force observer” because we can not comprehend the total output torque.

So in this section, we propose the control system whereby the error in hydraulic brake is compensated by electric motor. This is achieved by using the disturbance observer whose nominal model is the transfer function from total torque command to output acceleration. We named this compensate system “Nominalization of hydraulic brake by electric motor”.

3.1 Design of the control system

In this section, we design the controller which nominalizes the hydraulic brake. This controler compensates both modelling errors of vehicle dynamics and hydraulic brake. These errors are dealt with as a disturbance and compensated by the electric motors. Fig.3 shows the block diagram of the control system. There are many different ways to choose the nominal model’s

output. In this paper, we use (1) as a nominal model.

$$P_n(s) = \frac{\Delta a}{\Delta F_{total}} = \frac{1}{M + Mw} \quad (1)$$

Although it is theoretically possible to feedback all errors in modeling, for the purpose of improving ride comfort, we feedback the value of modeling error after subtracting air resistance and rotational resistance.

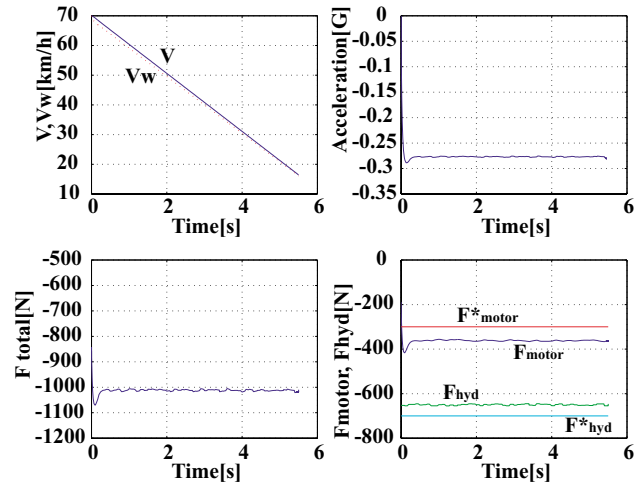
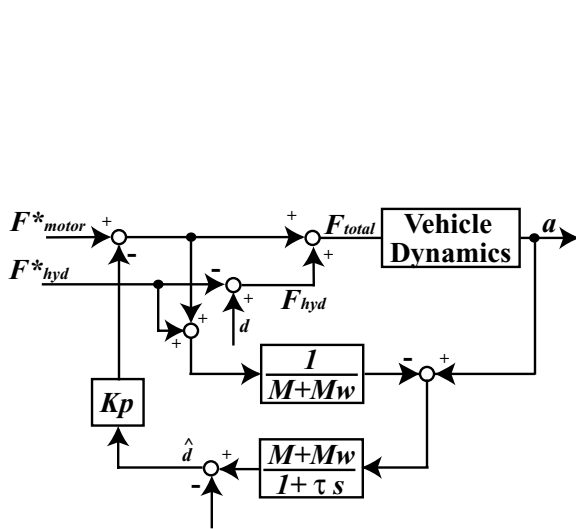


Fig. 3: Block diagram of control system for HEV Fig. 4: Simulation results of cooperative braking method

3.2 Simulation results

To prove the effectiveness of our proposed controller, we carried out some simulations. Fig.4 shows the simulation results. In this simulation, the braking torque commands are as follows, $F_{motor}^* = -300[N]$, $F_{hyd}^* = -700[N]$, and the disturbance in hydraulic brake is $d = 50 + \alpha[N]$, where α is noise. This situation indicates the hydraulic braking torque is smaller than its command. Fig.4 shows that the electric motor compensates for the errors in hydraulic brake. The electric motor produces the extra torque.

Figs.5 and 6 show the deceleration when error in hydraulic brake varies. The disturbance in Fig.5 consists of constant bias and white noise. Applying the controller, the difference of deceleration between no-disturbance and with-control is suppressed. The disturbance in Fig.6 consists of sine curve and white noise. In this situation, the difference of deceleration is also suppressed.

4 Hybrid-ABS

4.1 Problems in conventional ABS

HEV in actual market is equipped with the conventional ABS (Anti-lock Braking System) which works with hydraulic actuator. The conventional ABS activates the hydraulic actuator when the vehicle begins slipping. The hydraulic actuator has three modes; “increase pressure”, “keep pressure” and “decrease pressure”. The ABS controller switches among these three modes.

However the conventional ABS has some weak points. The first problem is undesired sound and vibration. The reasons of this problem is that the hydraulic actuator has only three modes. The most remarkable problem is that it dose not achieve good performance when the vehicle begins skidding. The reason of this problem is mainly in slow response of the hydraulic braking. This effect appears especially on low μ road.

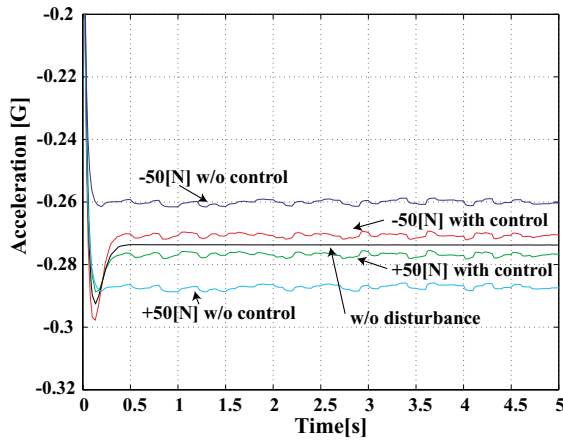


Fig. 5: Simulation results when DC disturbance is varied

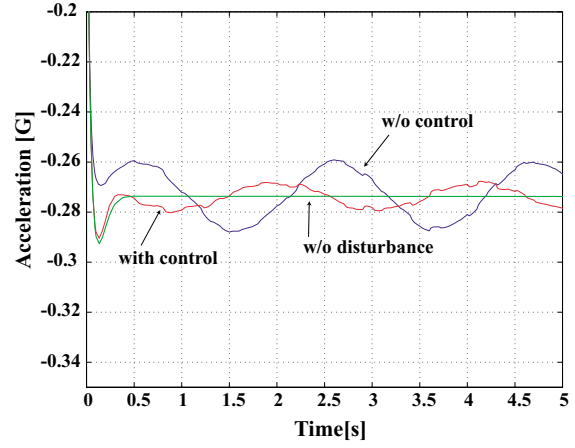


Fig. 6: Simulation results when AC disturbance is varied

4.2 The benefits and method of using electric motor for ABS

Generally speaking, the capacity of the electric motor in HEV is much smaller than that of hydraulic brake. The electric motor in HEV can not produce enough torque required for rapid braking. Hence, by combining these actuators, we can achieve both of size and quickness of output torque. Fig.7 shows the concept of this Hybrid-ABS. In this figure, $F_{brake} = F_{motor} + F_{abs}$ is comprised. As the electric motor has relatively smaller but more rapid torque output, it is responsible for high frequency band of F_{brake} . On the contrary, as the hydraulic brake has large, but slower torque output, it is responsible for low frequency band of F_{brake} .

Based on this concept of the cooperative control system, we named this braking system Hybrid-ABS. In the following sections, we propose three methods of implementing Hybrid-ABS. In 4.3.2, we construct Hybrid-ABS based on “PQ-method”, in 4.3.3, we use “Frequency selection by filter” and in 4.4, we construct based on “Model following control”. The outer loop of “PQ-method” and “Frequency selection by filter” is slip ratio control(S.R.C). “Model following control” is based on vehicle’s wheel velocity.

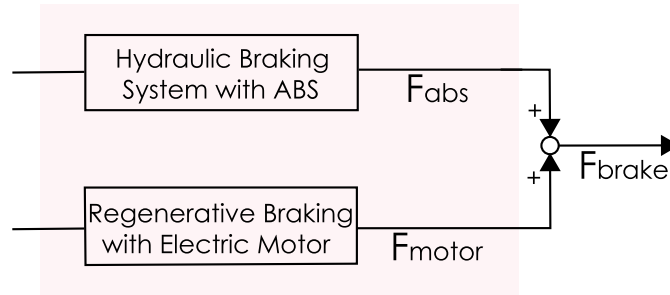


Fig. 7: Block diagram of Hybrid-ABS

4.3 Hybrid-ABS based on slip ratio λ

4.3.1 Design of slip ratio controller in braking

In this section, we apply the slip ratio controller as the main controller to prevent skid, which outputs the braking command to the Hybrid ABS. The effectiveness of the slip ratio controller is proved in [4]

Generally, slip ratio λ is given by (2).The vehicle motion equations in braking motion can be

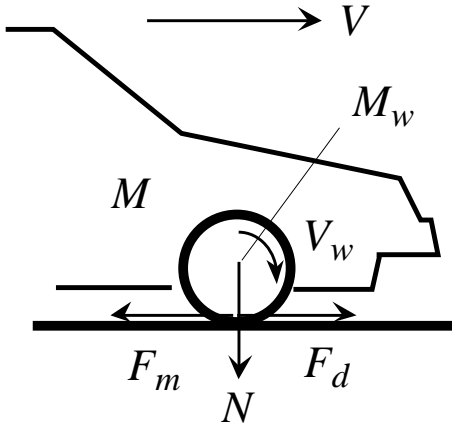


Fig. 8: Single wheel model

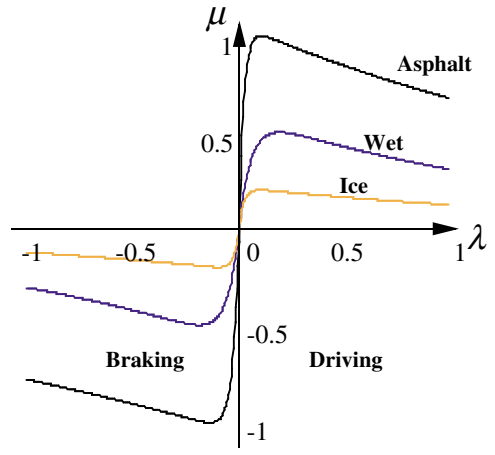


Fig. 9: $\mu - \lambda$ curve

obtained as (3).

$$\lambda = \frac{V_w, V}{\max(V_w, V)} \quad (2)$$

$$M_w \frac{dV_w}{dt} = F_m - F_d(\lambda) \quad (3)$$

$$M \frac{dV}{dt} = F_d \lambda \quad (4)$$

In these equations, V is the vehicle chassis velocity, V_w is the wheel velocity, M is the vehicle weight, M_w is the mass equivalent value of the wheel inertia, F_m is the force equivalent value of accelerating/decelerating torque, F_d is the driving/braking force between the wheel and the road surface, r and w are the wheel radius and rotational velocity, respectively. F_d is a function of λ (Slip Ratio) as is shown in Fig.9.

To design the slip ratio controller, (3) and (4) are too complicated, because the $\mu - \lambda$ curve (Fig.9) is non-linear.

The transfer function from F_{brake} to λ as in (5) is obtained by using around the operational point on $\mu - \lambda$ curve, the gradient of $\mu - \lambda$ curve a (6).

$$\frac{d\lambda}{dF_{brake}} = \frac{1}{aN_e} \frac{1}{1 + \tau_r s} \quad (5)$$

$$\tau_r = \frac{M_w V_{w0}}{a(1 + \lambda_0)N_e}, \quad a = \frac{d\mu}{d\lambda}, \quad \frac{1}{N_e} = \frac{1}{N} \frac{1}{1 + (1 + \lambda_0)P_w}, \quad P_w = \frac{M_w}{M} \quad (6)$$

In these equations, λ_0 is the slip ratio at the operational point.

Using the linearized vehicle equations (5) and (6), we design the slip-ratio controller as a P&I controller.

$$C(s) = K_P + \frac{K_I}{s} \quad (7)$$

Applying this controller, the transfer function from λ^* to λ is described as

$$\begin{aligned} \frac{\lambda}{\lambda^*} &= \frac{C(s)P(s)}{1 + C(s)P(s)} \\ &= \frac{\frac{K_P}{aN_e\tau_r} s + \frac{K_I}{aN_e\tau_r}}{s^2 + \left(\frac{K_P}{aN_e\tau_r} + \frac{1}{\tau_r}\right)s + \frac{K_I}{aN_e\tau_r}} \end{aligned} \quad (8)$$

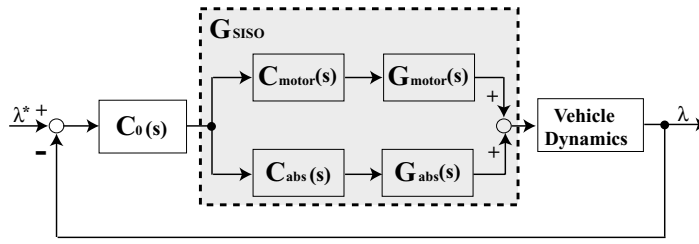


Fig. 10: Block diagram of PQ-method applied to ABS

If we assign the pole of the control system as s_0 , K_P and K_I are determined as (9) and (10). Further (9) and (10) have V_w as a parameter, so we change (9) and (10) as the real V_w change.

$$K_P = -aN_e - \frac{2s_0 M_w V_w}{1 + \lambda^*} \quad (9)$$

$$K_I = \frac{s_0^2 M_w V_w}{1 + \lambda^*} \quad (10)$$

4.3.2 PQ-method

The actuators of Hybrid ABS are the electric motor with small but rapid output and the hydraulic brake with large but slow output. This combination of actuators is similar to that of the dual stage actuator system of hard disc drive system(HDD). This system consists of a coarse actuator(Voice Coil Motor) and a fine actuator(PieZoelectric Transducer, PZT). Several methods are proposed as a control strategy of dual stage actuator system. For example, Master-Slave Control and Parallel Control. The effectiveness of these control strategies have been proved[6][7][8]. In this paper, we design Hybrid-ABS based on one of the novel design methods “PQ-method”.

Controller Design PQ-method is one of the “Parallel Control”. Using this method, we can construct the controller so that it prevents destructive interference between electric motor and hydraulic brake. Fig.10 is the block diagram of the PQ-method for HEV. In this figure, G_{motor} and G_{abs} are the dynamics of the electric motor and hydraulic brake respectively. When we design the controller, these factors are approximated to first order delay. C_{motor} and C_{abs} are each actuator’s controller. G_{SISO} in Fig.10 is described as (11).

$$G_{SISO} = C_{motor}G_{motor} + C_{abs}G_{abs} \quad (11)$$

In Fig.10, P and Q are defined by (12).

$$P = \frac{G_{abs}}{G_{motor}}, \quad Q = \frac{C_{abs}}{C_{motor}} \quad (12)$$

The aim of this controller is that the electric motor will be responsible for the high frequency part and hydraulic brake for the lower frequency part. Therefore $|PQ|$ in (12) are determined as in (13)–(15).

$$|PQ| \ll 1 \quad (13)$$

(High frequency region : Braking torque is generated mainly by electric motor)

$$= 1 \quad (14)$$

(Middle frequency region : Braking torque is shared evenly between two actuators)

$$\gg 1 \quad (15)$$

(Low frequency region : Braking torque is generated mainly by hydraulic brake)

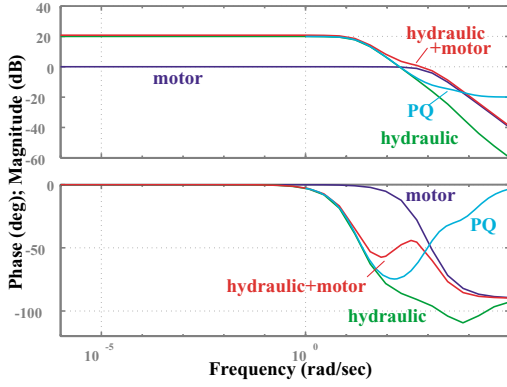


Fig. 11: Bode diagram of hydraulic and electric actuators

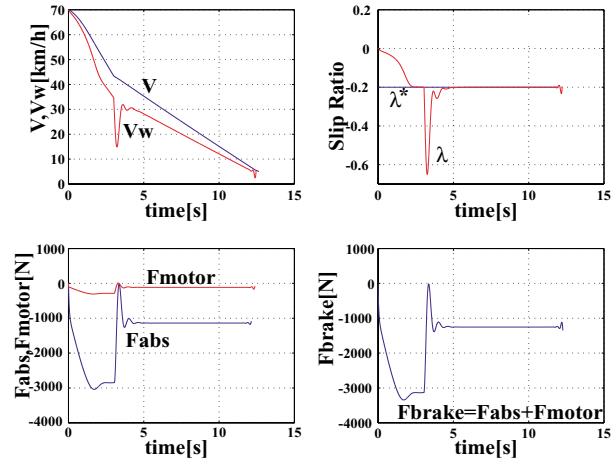


Fig. 12: Simulation results of PQ-method

P depends on the dynamics of the plant. P is described as follows,

$$P = \frac{G_{abs}}{G_{motor}} = \frac{\frac{1}{1+\tau_{abs}s}}{\frac{1}{1+\tau_{motor}s}} \quad (16)$$

Next, we design Q to satisfy equations (13)–(15). And we should avoid the situation where the phase of these astuator is particularly different when $|PQ| = 1$. In this case, there is destructive interference between two actuators. To prevent such interference, the phase margin of PQ should be greater than $60[degree]$.

$$Q = K_P \frac{1+Ts}{1+\alpha Ts} \quad (17)$$

After Q has been selected, we select both C_{abs} and C_{motor} to be realizable and satisfy (17). In this case, Q is realizable, $C_{motor} = 1$ is a reasonable choice. C_{motor} and C_{abs} are as follows,

$$C_{motor} = 1, \quad C_{abs}(s) = K_P \frac{1+Ts}{1+\alpha Ts} \quad (18)$$

Fig.11 is the bode diagram of the designed controller. But as shown in Fig.10, the input of the G_{SISO} is not λ^* but F_{brake}^* . So we must design the controller from λ^* to F_{brake}^* . Here, we use the slip-ratio controller(7).

Simuration results To prove the effectiveness of the cooperative controller which is based on PQ-method. We carried out simulations. Fig.12 is the simulation results. In this simulation, sudden brake is applied on slippery low μ road. The value of the μ_{peak} changed from 0.5 to 0.3 at 3[s]. The movement of λ is stable after changing the μ_{peak} .

4.3.3 Frequency selection by filter

In the previous section, we designed the Hybrid-ABS based on PQ-method. Using this method, we can construct the controller which prevents the harmful interference. But this controller is still too complex. When we design the outer loop of chassis control, the complexity of Hybrid-ABS will be a problem.

In this section, we propose much simple controller for Hybrid-ABS just to separate the frequency region of the two actuators.

Design of controller In this controller, we presuppose the dynamics of each actuators as follows.

$$G_{motor}(s) \cong 1, \quad G_{abs}(s) \cong \frac{1}{1+\tau_{abs}s} \quad (19)$$

And we presuppose G_{SISO} in Fig.10 as follows.

$$G_{SISO} = C_{motor}G_{motor} + C_{abs}G_{motor} = 1 \quad (20)$$

From these planning, the difference between G_{SISO} and C_0 is clear. G_{SISO} decides the distribution of the active frequency band, C_0 decides the control of slip ratio λ . Another interest of the braking is energy regeneration. In this controller, we can set the regenerative rate by adjusting the gain of the electric motor easily. C_{motor} and C_{abs} are described as

$$C_{motor}(s) = \frac{\tau s + gain}{\tau s + 1} \quad (21)$$

$$C_{abs}(s) = \frac{1 - gain}{\tau s + 1} (1 + \tau_{abs}s) \quad (22)$$

Fig.4.3.3 shows the bode diagram of this system. In this case, the regenerative rate is set at 10%.

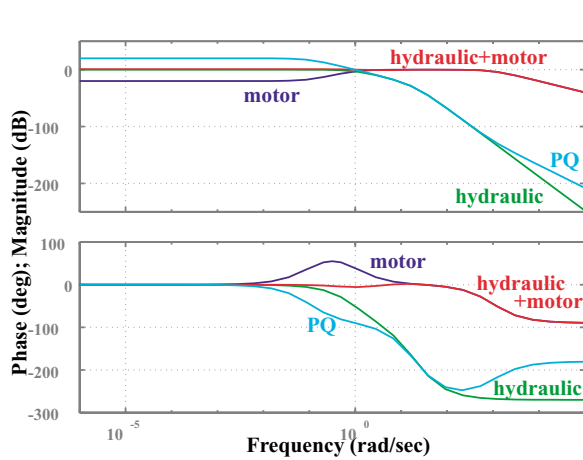


Fig. 13: Bode diagram for the case of 10% energy regeneration

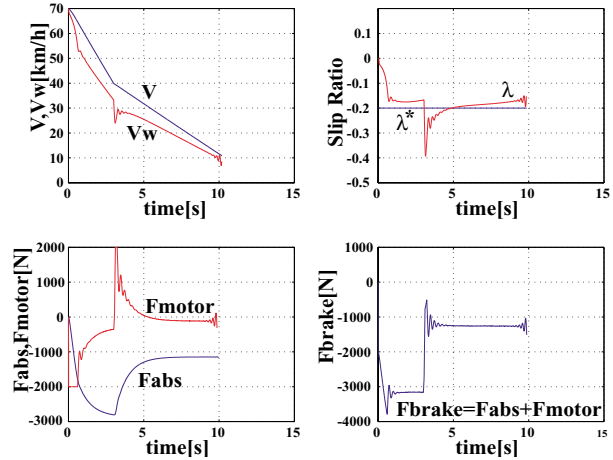


Fig. 14: Simulation results of filter-method

Simulation results To prove the effectiveness of the proposed controller, we carried out simulations. Fig.14 is the simulation results. Simulation condition is the same as that of PQ-method(Fig.12). Compared with Fig.12, the role differentiation of each actuator is clearer. When the vehicle begins slipping suddenly(at 3[s] in Fig.14), the electric motor outputs forward torque. From this motion, the vehicle can recover from slip motion quickly.

4.4 Hybrid-ABS based on vehicle's wheel velocity

In the previous sections, we proposed several control methods. Their methods are based on slip ratio λ . But to realize slip ratio control, we must grasp the vehicle velocity in real-time. In this section, we propose the control method without using vehicle chassis velocity.

4.4.1 Design of controller

The vehicle dynamics during the braking can be linearized as (23)–(25).

$$P(s) = \frac{1}{(M_w + M(1 + \lambda_0))s} \frac{\tau_w s + 1}{\tau_a s + 1} \quad (23)$$

$$\tau_a = \frac{M_w V_{w0}}{aN} \frac{M}{M(1 + \lambda_0) + M_w} \quad (24)$$

$$\tau_w = \frac{\tau_w s + 1}{\tau_a s + 1} \quad (25)$$

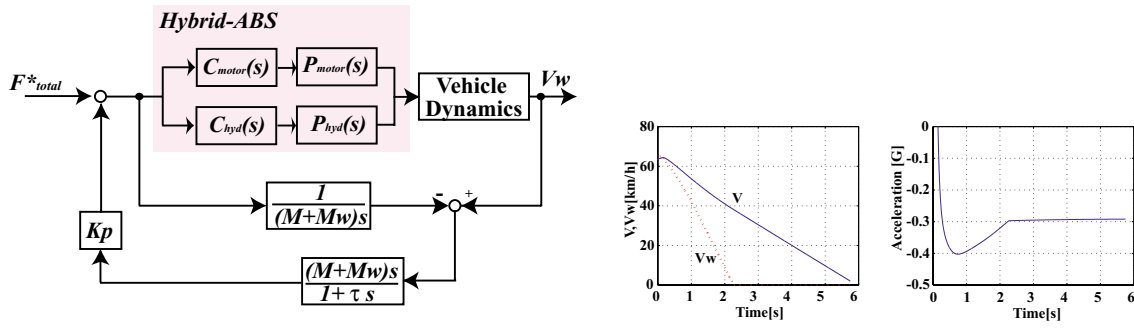


Fig. 15: Block diagram of Hybrid-ABS(based on Fig. 16: Simulation results of MFC-Hybrid-ABS(Without Control)

If we approximate skidding condition as $\lambda = -1$ and adhesive condition as $\lambda = 0$, (23)–(25) becomes as follows,

$$P_{adh} = \frac{1}{(M + M_w)s} \quad (26)$$

$$P_{skid} = \frac{1}{M_w s} \quad (27)$$

This type of controller is called “MFC(Model Following Control)” and proposed as anti-skid control method for Pure EV[5]. If we apply MFC to HEV, we must be concerned with some factors for example time delay of the hydraulic line. Using the control method as **4.3.3**, we can regard $C_{motor}P_{motor} + C_{hyd}P_{hyd} = 1$. Therefore we do not have to consider these factors. Fig.15 shows the block diagrams of our proposed method.

4.4.2 Simulation results

We carried out simulations to prove the effectiveness of the Hybrid-ABS method which is based on MFC. In the simulations, sudden brake is applied on slippery low μ road. μ_{peak} is 0.4. Fig.16 shows the results without control. In this case, the vehicle's wheel locks at 2.3[s]. Fig.17 shows the results with control. The wheel does not lock. And the limiting value of the braking force at this road is 1274[N]. In this simulation, the controlled vehicle's braking force is about 1200[N]. This result is good. Fig.18 shows the comparison of deceleration, when K_P is varied.

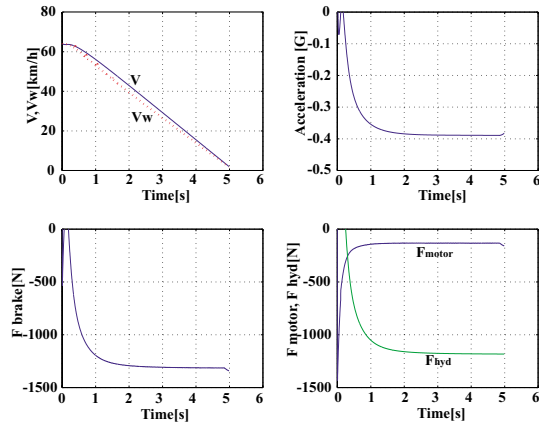


Fig. 17: Simulation results of MFC-Hybrid-ABS($K_p=10$)

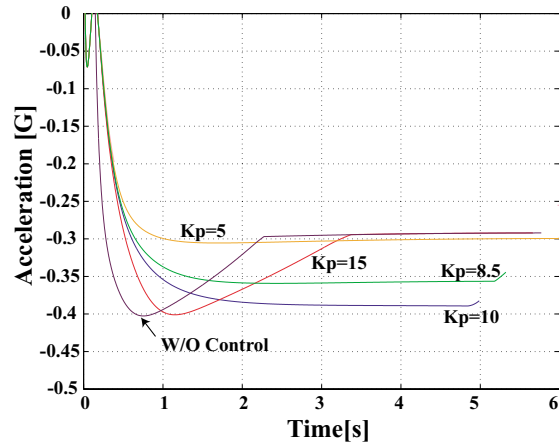


Fig. 18: Comparison of braking acceleration, when K_P is varied

5 Experiments of Hybrid-ABS

5.1 General outline of experiments

We carried out basic experiments using “UOT Electric MarchII” as shown in Fig.19. The applied control method is filter-method which is introduced in 4.3.3. But the limitation of “UOT Electric MarchII”, is that we cannot control hydraulic brake freely. So we simulated the hydraulic brake's dynamics on computer. Fig.20 is the block diagram of the experiment. And we used real hydraulic brake at the same time, because of the power limit of the electric motor. The experimental condition is described as follows,



Fig. 19: UOT Electric March II

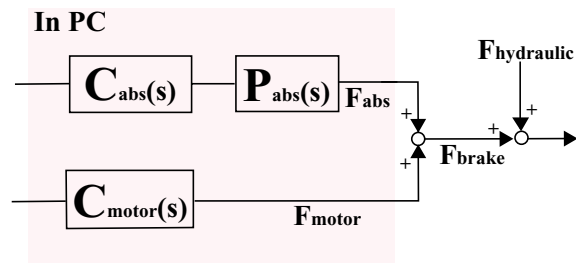


Fig. 20: Block diagram of experiments

- Initial vehicle's velocity is 60[km/h].
- The “UOT Electric MarchII” did rapid braking at low μ road.
- 5th wheel is used to measure the vehicle's velocity.
- μ_{peak} of the experimental road is about 0.4.

5.2 Experimental results

Figs.21-23 show the experimental results. Without control, the wheel velocity rapidly decreased and the vehicle's wheels were soon locked(Fig.21). Fig.22 is driven by professional test driver. This result is near optimal. But this is too difficult to imitate for normal drivers. On the contrary, the slip motion was prevented when our proposed method was applied(Fig.23). And the vehicle stopped safely. The role differentiation of each actuator was achieved. One of the remaining problems is the oscillation of the slip ratio λ . It is probably due to the design of controller's parameters. We will solve this problem in our next experiment.

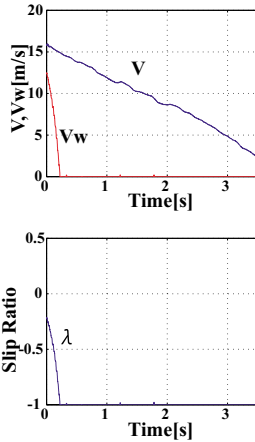


Fig. 21: Without control

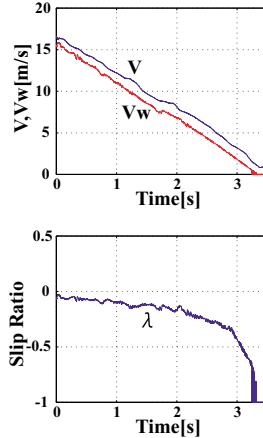


Fig. 22: By test driver

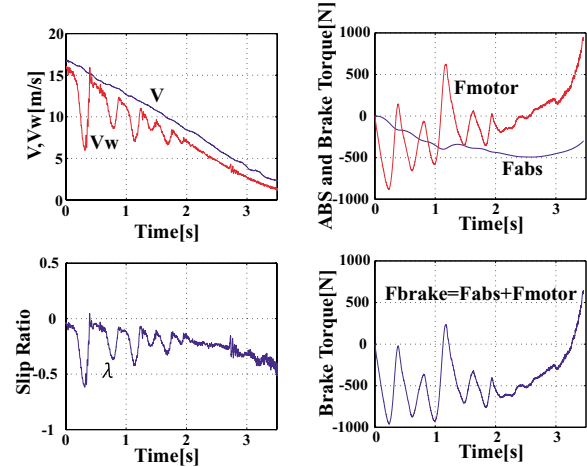


Fig. 23: Our proposed method Hybrid-ABS

6 Conclusion and future researches

In this paper, we proposed an integrated vehicle motion control for HEV. This system consists of Hybrid-ABS and nominalization of hydraulic brake. We proposed three methods of implementing Hybrid ABS, based on "PQ-method", "Frequency selection by filter" and "Model following control" and proved that Hybrid ABS improves the performance of ABS through computer simulation and experiments. Further, through nominalization of the hydraulic brake, we can eliminate uncertainty from the hydraulic brake's output. The effectiveness of this method was shown through computer simulations. The most remarkable point of our research is in the utilization of electric motor's advantage for HEV: quick, accurate and bi-directional torque generation. However at present, we are unable to control the hydraulic brake output of our experimental vehicle and it is emulated through the onboard computer controllers. We will therefore carry out further experiments using a real HEV in the near future.

References

- [1] Toyota Internet Drive, <http://www.toyota.co.jp>
- [2] Honda Motor Company Homepage, <http://www.honda.co.jp>
- [3] Hiroyuki Watanabe, "The Keyword of for the 21st Century -Hybrid-", The opening session of EVS17, 2000.
- [4] Y. Hori, Y. Toyoda and Y. Tsuruoka, "Traction control of electric vehicle: Basic experimental results using the test ev "UOT Electric March", IEEE Trans. Ind. Applicat., vol.34, No.5, pp.1131-1138, 1998.
- [5] Shin-ichiro Sakai, Hideo Sado and Yoichi Hori, "Novel Skid Detection Method without Vehicle Chassis Speed for Electric Vehicle", JSAE Review (Elsevier Science), Vol.21, No.4, pp.503-510, 2000.
- [6] Ding J., Numasato H., Tomizuka M., "Single/Dual-rate Digital Controller Design for Dual Stage Track Following in Hard Disk Drives", AMC2000-NAGOYA, pp. 80-85, 2000.
- [7] L.-S. Fan, H. H. Otesen, T. C. Reiley, R. W. Wood, "Magnetic recording head positioning at very high track densities using a microactuator-based, two-stage servo system", 42, 3, pp. 222-233, 2000.
- [8] Steven J.Schroeck, William C.Messner., "On Controller Design For Linear Time-Invariant Dual-Input Single-Output Systems", AACC1999, pp. 4122-4126, 1999.

Authors



Takahiro Okano, Master's degree candidate / The University of Tokyo,
7-3-1 Hongo, Bunkyo Tokyo 113-8656, Japan;
Phone: +81-3-5841-6678, Fax: +81-3-5841-8573, E-mail : okano@hori.t.u-tokyo.ac.jp
URL: www.hori.t.u-tokyo.ac.jp/2000/okano

He was born in Aichi, Japan in 1978. He received the B.S degree in electrical engineering from University of Tokyo in 2001. He will be working at Toyota Motor Corporation from April 2003.



Shin-ichiro Sakai, Ph.D. / The Institute of Space and Astronautical Science,
3-1-1, Yoshinodai, Sagamihara, Kanagawa, Japan;
Phone: +81-42-759-8308, Fax: +81-42-759-8473, E-mail : sakai@pub.isas.ac.jp
URL: www.hori.t.u-tokyo.ac.jp/997/sakai

He received the Ph.D. degrees in electrical engineering from the University of Tokyo, in 1995, 1997 and 2000, respectively. In 2000 he worked as JSPS Research Fellow in the University of Tokyo, and since 2001 he is a research associate in The Institute of Space and Astronautical Science.



Toshiyuki Uchida, Technical Staff / The University of Tokyo
7-3-1 Hongo, Bunkyo Tokyo 113-8656, Japan;
Phone: +81-3-5841-6678, Fax: +81-3-5841-8573, E-mail : uchida@hori.t.u-tokyo.ac.jp
URL: www.hori.t.u-tokyo.ac.jp/staff/uchida

He has worked at the University of Tokyo as a technical staff since 1986.



Yoichi Hori, Ph.D. / The University of Tokyo,
7-3-1 Hongo, Bunkyo Tokyo 113-8656, Japan;
Phone: +81-3-5841-6678, Fax: +81-3-5841-8573, E-mail : hori@hori.t.u-tokyo.ac.jp
URL: www.hori.t.u-tokyo.ac.jp/staff/hori

He received the Ph.D. degrees in electrical engineering from the University of Tokyo in 1983. He joined the Dept. of Elec. Eng. at the Univ. of Tokyo as a research associate in 1983. Since 2000, he has been a professor.